The Journal of Chemical Physics

Pattern of property extrema in supercooled and stretched water models and a new correlation for predicting the stability limit of the liquid state

Cite as: J. Chem. Phys. **150**, 064503 (2019); https://doi.org/10.1063/1.5078446
Submitted: 25 October 2018 . Accepted: 19 January 2019 . Published Online: 12 February 2019

Betul Uralcan, Folarin Latinwo, Pablo G. Debenedetti, and Mikhail A. Anisimov

The Journal of Chemical Physics ARTICLE scitation.org/journal/jcp

Pattern of property extrema in supercooled and stretched water models and a new correlation for predicting the stability limit of the liquid state

Cite as: J. Chem. Phys. 150, 064503 (2019); doi: 10.1063/1.5078446
Submitted: 25 October 2018 • Accepted: 19 January 2019 •
Published Online: 12 February 2019

Betul Uralcan,[1] Folarin Latinwo,[1,a)] Pablo G. Debenedetti,[1] and Mikhail A. Anisimov[2,b)]

AFFILIATIONS

[1]Department of Chemical and Biological Engineering, Princeton University, Princeton, New Jersey 08544, USA
[2]Department of Chemical and Biomolecular Engineering and Institute for Physical Science and Technology, University of Maryland, College Park, Maryland 20742, USA

[a)]**Current address:** Synopsys Technology, 1301 South Mopac Expressway, Austin, Texas 78746, USA.
[b)]**Electronic mail:** anisimov@umd.edu

ABSTRACT

Water exhibits anomalous behavior in its supercooled region. A widely invoked hypothesis to explain supercooled water's thermodynamic anomalies is the existence of a metastable liquid-liquid transition terminating at a critical point. In this work, we analyze previously published and new simulation results for three commonly used molecular water models (ST2, TIP4P/2005, and TIP5P) that support the existence of the metastable liquid-liquid transition. We demonstrate that a corresponding-states-like rescaling of pressure and temperature results in a significant degree of universality in the pattern of extrema loci of the density, isothermal compressibility, and isobaric heat capacity. We also report, for the first time, an intriguing correlation between the location of the liquid-liquid critical point, the rescaled locus of density extrema, and the stability limit of the liquid state with respect to the vapor. A similar correlation is observed for two theoretical models that also exhibit a second (liquid-liquid) critical point, namely, the van der Waals and lattice-gas "two-structure" models. This new correlation is used to explore the stability limit of the liquid state in simultaneously supercooled and stretched water.

I. INTRODUCTION

Despite being ubiquitous and essential for life, liquid water is still incompletely understood, especially in its supercooled and stretched metastable states.[1–21] A striking anomaly is the existence of a locus of density extrema, which continues into supercooled and deeply stretched (negative pressures) states.[22–25] The observed extrema loci of response functions, such as isothermal compressibility (κ_T) and isobaric heat capacity (C_P), are strongly correlated with the shape of the density extrema locus.[22,23]

One possible explanation for water's anomalous behavior is the existence of a metastable first-order phase transition involving two distinct liquid phases that terminates at a liquid-liquid critical point (LLCP).[5,18] This liquid-liquid transition is considered to be a special case of fluid polyamorphism,[25] a phenomenon that has been either found or hypothesized in a broad range of materials including metallic hydrogen,[26–28] silicon,[29–31] silica,[32,33] carbon,[34] cerium,[35] and phosporous.[36] Although experimental evidence consistent with polyamorphism exists for supercooled water,[6,37] a definitive proof is still lacking. Computer simulations, on the other hand, have shown that some molecular models of water exhibit liquid-liquid separation at deeply supercooled conditions.[22,38–48] In tetrahedral systems, regardless of the existence or non-existence of the liquid-liquid separation (e.g., mW,[49–51] mTIP4P,[50] ST2,[52]

TIP4P/2005,[53] TIP5P,[54] silicon,[30,31,55] silica,[32,33] and germanium[56]), there is an underlying characteristic pattern of extrema lines for thermodynamic properties. The most well-known is the line of density extrema, whose existence suggests a competition between low-density and high-density structures in the same liquid.

The existence of the liquid-vapor and liquid-liquid transitions in a single-component fluid implies the possibility of a correlation between the pattern of extrema lines associated with the liquid-liquid transition and the stability limit of the liquid with respect to the vapor. A schematic phase diagram of a single-component fluid exhibiting both liquid-vapor and liquid-liquid phase transitions[25] is shown in Fig. 1. The possibility for such a fluid to crystallize is not shown in the phase diagram; however, if crystallization preempts polyamorphism, the liquid-liquid phase transition (LLPT) would simply be metastable with respect to crystallization. We also note that, in this particular example, the lower branch of the density extrema line, like the low-temperature part of the liquid-vapor spinodal (LVS), is located at negative pressures (stretched liquid state). The question thus arises as to whether there is any correlation between the extrema pattern and the stability limit of the liquid with respect to the vapor.

In this work, we analyze the pattern of extrema lines observed in three commonly used molecular water models (ST2, TIP4P/2005, and TIP5P) that exhibit a metastable liquid-liquid transition. We use earlier published data for ST2 (long-range electrostatic interactions are treated with the reaction field method[57]) and TIP4P/2005,[44,58] and present new simulation data for TIP5P (see the details in the supplementary material). Rescaling the pressure and temperature coordinates for all these models results in a significant degree of universality in the pattern of extrema lines of the density, isothermal compressibility, and isobaric heat capacity. We also uncover a correlation between the location of the liquid-liquid critical points, the rescaled locus of thermodynamic property extrema, and the stability limit of the liquid state with respect to the vapor. We discuss how this trend could be utilized for the prediction of the stability limit of the liquid state in real supercooled and stretched water, at conditions where experimental data are currently unavailable. We demonstrate a similar correlation for two generic fluid models that also exhibit a liquid-liquid critical point, namely, the "two-state" van der Waals model and the "two-state" lattice-gas model.[25] We also discuss the possibility of applying the rescaling procedure to other tetrahedral systems.

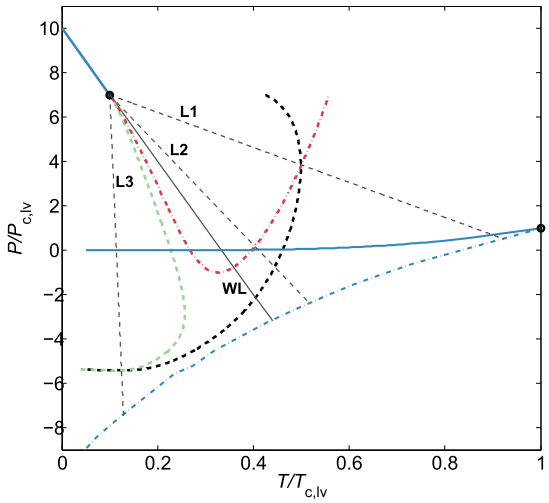

FIG. 1. Generic phase diagram for a polyamorphic fluid (calculations for the two-state van der Waals model described by Anisimov *et al.*[25]). $P_{c,lv}$ and $T_{c,lv}$ are the pressure and temperature of the liquid-vapor critical point (LVCP). The blue curves are vapor-liquid and liquid-liquid first-order transitions ending at the LVCP and the liquid-liquid critical point (LLCP), respectively. The thin black line is the Widom line (WL), defined in the text. The blue dotted-dashed curve is the liquid branch of the liquid-vapor spinodal (LVS). The black, red, and green dashed curves are loci of density, isothermal compressibility and isobaric heat capacity extrema, respectively. The three thin black dashed lines (L1, L2, and L3) are selected paths connecting the LLCP and the LVS (see Sec. III).

II. SEARCHING FOR UNIVERSALITY IN THE PATTERN OF THE PROPERTY EXTREMA

For the analysis of property extrema in molecular water models in the supercooled and stretched regions, we use molecular dynamics simulations of the ST2[38,57,60] and TIP4P/2005 water models[44,58] and report new data for the TIP5P model. The information on the property extrema in the ST2 and TIP4P/2005 models as well as for the previously unpublished TIP5P model is presented in the supplementary material. In addition to the molecular water models, we also consider preliminary results for a two-structure equation of state (TSEOS) fit to experimental data for real metastable and stretched water.[59]

Figure 2 depicts the extrema of density, isothermal compressibility (computed along isobars), and isobaric heat capacity (computed along isotherms) for three molecular water models that exhibit a liquid-liquid phase transition terminating at a critical point, namely, ST2,[38,57,60] TIP4P/2005,[44,58] and TIP5P (supplementary material), and for real water obtained from the TSEOS fit to existing experimental data.[59] The stability limit of the liquid with respect to the vapor gives the lower limit of the phase diagram of liquid water. This limit is *thermodynamically* defined as a locus of divergent isothermal compressibility (blue dotted-dashed curve in Fig. 1), but it is not directly attainable from the experiment. The *kinetic* stability limit, on the other hand, can be directly observed in simulations, defined as the locus of spontaneous vapor cavity formation in the liquid[61] (thin solid lines in Fig. 2). Thus, for the molecular water models, we show the kinetic stability limit of the liquid with respect to the vapor (thin solid lines in Fig. 2), which will be used to predict the stability limit for real water in Sec. III.

For the systems that we consider, the loci of density, isothermal compressibility and isobaric heat capacity extrema, and the liquid-vapor spinodal exhibit a strikingly similar pattern.[23,50,51,57,62] The location of the critical points and the thermodynamic property extrema are clearly system-dependent, but the various extrema loci exhibit many

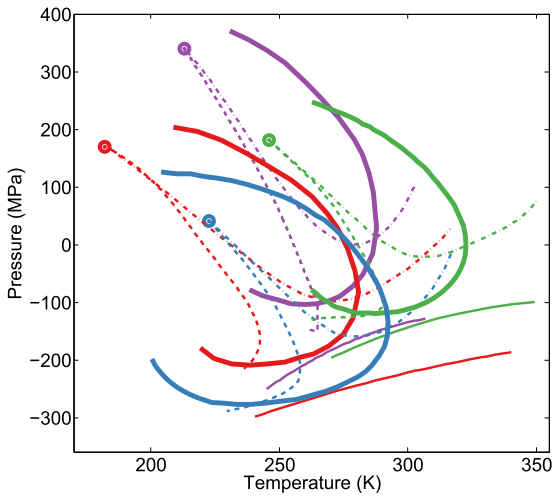

FIG. 2. Extrema lines of various thermodynamic properties for different systems [green for ST2,[40] red for TIP4P/2005,[44,58] purple for TIP5P (supplementary material), and blue for real water, predicted by a fit to available experimental data[59]]. The thick solid, dashed, and dotted/dashed curves represent the loci of density, isobaric heat capacity (computed along isotherms), and isothermal compressibility (computed along isobars) extrema, respectively. The circles indicate the liquid-liquid critical points (LLCP). The thin solid lines are the cavitation lines which are observed in simulations for the water models.

common features imposed by thermodynamics.[23,62] In particular, the loci of response function maxima merge asymptotically at the LLCP. The density shows maxima at positive pressures (temperature of maximum density, TMD). The TMD first shifts to higher temperatures as the pressure is lowered, however, upon further decrease in pressure, it eventually retraces after reaching a maximum temperature ("nose") and terminates when it meets the locus of minimum densities (TmD). As required by thermodynamic constraints for the case of a monotonically increasing liquid-vapor spinodal,[23,57] the locus of isothermal compressibility extrema intersects the TMD line's "nose." Also, the point at which the locus of density maxima joins the locus of density minima is a point along the locus of extrema of C_P, measured along isotherms.[23,57,62]

A corresponding-states-like[63,64] rescaling of the patterns of property extrema with an eye towards a unified description could make the observed phenomena more informative and predictive. A preliminary attempt to collapse the extrema lines for two models, TIP4P/2005 and ST2, was made by Biddle.[65] In this work, we suggest a different, though conceptually similar procedure for rescaling the temperature and pressure coordinates for the systems in Fig. 2. Specifically, the rescaling analysis in this work is guided by the generic two-state formulation of polyamorphic fluids in Anisimov *et al.*,[25] where the Gibbs energy difference between distinct but interconvertible states is affected by three parameters, namely, the change in energy, entropy, and volume. In the linear approximation, the Gibbs energy difference between the two interconvertible states, B and A, reads[25]

$$G_{BA}(P, T) = \lambda + \alpha P + \beta T, \tag{1}$$

where the coefficients λ, α, and β represent the changes (in the linear approximation) of energy, volume, and entropy, respectively. The phase transition line and the Widom line are defined as $\lambda + \alpha P + \beta T = 0$ with a constant slope $dP/dT = dS_{BA}/dV_{BA} = -\beta/\alpha$. This is why the rescaling requires at least three transformation steps: independently rescaling the temperature, the pressure, and accounting for a coupling between P and T along the Widom line or along any other characteristic line emanating from the LLCP. The temperature and pressure coordinates are rescaled to account for the correlation between the liquid-liquid critical points and the density extrema loci, such that

$$T' = \frac{T - T_c}{T_{max} - T_c} \tag{2}$$

and

$$P' = \frac{P - P(T_{max})}{P_c - P_{min}}, \tag{3}$$

where T_c and P_c are the coordinates of the LLCP, T_{max} is the maximum temperature on the TMD line, and P_{min} is the minimum pressure on the TMD line. This rescaling fixes the coordinates of the "nose" of the TMD at (1, 0) in the scaled temperature/pressure plane, in analogy to the usual practice of fixing the scaled coordinates of the critical point in corresponding states representations of the coexistence region.[63] Equations (2) and (3) also fix the vertical distance between the critical point and the point of minimum pressure along the TMD (P_{min}) to be equal to 1 in reduced pressure units. As depicted in Fig. S8, this rescaling already provides an appreciable collapse for the systems considered in this work (compare with Fig. 2). The final transformation (rotation of the coordinates) was made by rotating the extrema loci to superimpose the line connecting the LLCP and the "nose" of the TMD line (L1 in Fig. 1), thus setting dP/dT constant along this line and accounting for the different dS_{BA}/dV_{BA} scales. Specifically, we kept the extrema lines for the TSEOS fit for real water as in Fig. S8, and rotated the molecular water models about the TMD "nose", so as to attain a common slope of the line joining the LLCP and the TMD nose. The resulting rotated coordinates are given by

$$\begin{bmatrix} \tilde{T} \\ \tilde{P} \\ 1 \end{bmatrix} = \begin{bmatrix} \cos\theta & -\sin\theta & 1-\cos\theta \\ \sin\theta & \cos\theta & -\sin\theta \\ 0 & 0 & 1 \end{bmatrix} \begin{bmatrix} T' \\ P' \\ 1 \end{bmatrix}, \tag{4}$$

where θ is the rotation angle around the "nose" of the TMD line [see Table S2 for θ values and Eq. (S3) to read back (T', P') from ($\tilde{T}$, $\tilde{P}$)]. By construction, this step aligns the LLCPs along a straight line (see the insert in Fig. 3). We note that the rotation angles for these systems are small since all of them are models representing the same substance (i.e., water). It is for this reason that rescaling without rotation leads to a satisfactory level of collapse in this analysis (Fig. S8), but rotation would be essential for generalization to models with considerably different L1 slopes (see Fig. S11).

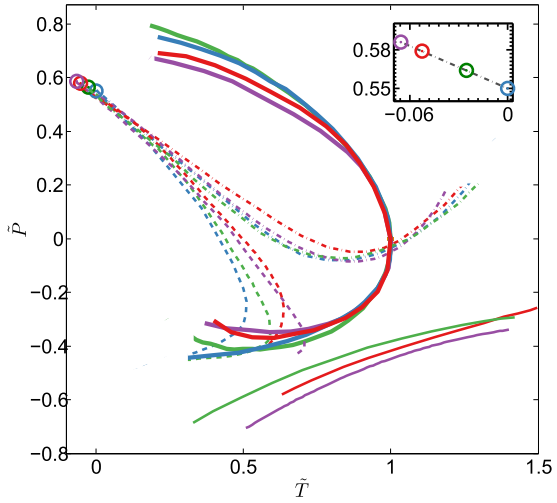

FIG. 3. Extrema lines of various thermodynamic properties in the rescaled coordinates [green for ST2,[40] red for TIP4P/2005,[44,58] purple for TIP5P (supplementary material), and blue for real water predicted by a two-structure equation of state[59]]. The thin solid lines are the cavitation lines which are observed in simulations for the water models. In the rescaled coordinates, the LLCPs lie along a straight line (see the inset).

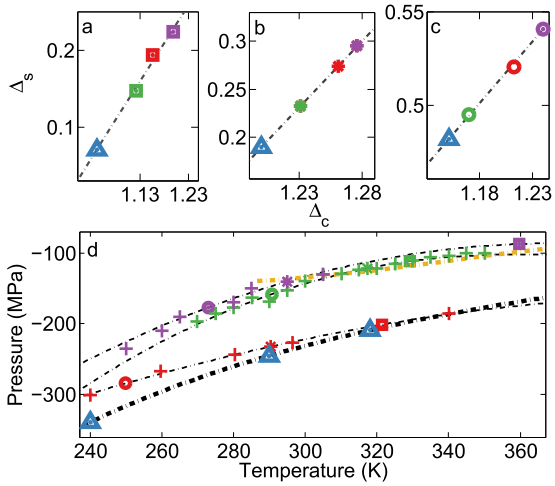

FIG. 4. The correlation between the location of the liquid-liquid critical points, the loci of density extrema, and liquid stability lines in rescaled coordinates. The parameter Δ_c is the distance between LLCP and the following points along the TMD locus: (a) intersection with the locus of C_P extrema, path L3 in Fig. 1; (b) intersection with the point on the TMD locus having a pressure that is equal to the average of P_{min} and $P(T_{max})$, path L2 in Fig. 1; (c) intersection with the locus of κ_T extrema, path L1 in Fig. 1. The parameter Δ_s is the distance between the stability limits of water with respect to its vapor and the above-defined corresponding points on the density extrema locus along the same paths. (d) Consistency of computed liquid-vapor stability limits with the linear correlations between Δ_c and Δ_s. The crosses [green for ST2,[40] red for TIP4P/2005,[44,58] purple for TIP5P (supplementary material)] are kinetic stability limits (cavitation) obtained from simulations. Circles, stars, and squares are obtained from the correlations for molecular water models [green for ST2,[40] red for TIP4P/2005,[44,58] purple for TIP5P (supplementary material)], and the dotted-dashed lines are quadratic fits to the symbols. Blue triangles are the prediction of the kinetic stability limit for real water from the above correlations, and the black dotted-dashed line is a quadratic fit to the data. The yellow dotted-dashed line is the experimental kinetic stability limit given in Qiu *et al.*[19]

The results in final rescaled coordinates are shown in Fig. 3. It is remarkable that this rescaling achieves the degree of collapse one sees in going from Fig. 2 to Fig. 3. The shape of the TMD locus is not constrained by our scaling, and it can be seen from Fig. 3 that (i) this locus departs from "universality" below $\tilde{T} \approx 0.75$, both at high and low pressures; (ii) there is better collapse for the loci of compressibility extrema than for the corresponding heat capacity extrema; (iii) the kinetic limits of stability with respect to the vapor exhibit interesting collapse, even if unconstrained by the choice of scaling. These observations apply to the molecular water models considered here (ST2, TIP4P/2005, and TIP5P), and there is no implication as to their generality. In sum, the choice of proper scaling accomplishes a very satisfactory degree of collapse, including in features that are not constrained by scaling (e.g., kinetic limits of stability), suggesting "universality" in the overall picture. Although some global features imposed by thermodynamics are model-independent (e.g., the intersections between the TMD and the heat capacity and compressibility extrema, the former defining P_{min} and the latter defining T_{max}, as can be seen in Fig. 2), achieving satisfactory collapse through scaling is a non-trivial result.

III. CORRELATION WITH THE STABILITY OF THE LIQUID STATE

The rescaling of pressure and temperature coordinates brings to light an intriguing correlation between the liquid-liquid critical point, the TMD line, and the kinetic liquid-vapor stability limit for molecular water models. Figures 4(a)–4(c) show the distance, in scaled coordinates, from the LLCP to the TMD line (Δ_c) displayed against the distance from the TMD line to the kinetic limit of liquid-vapor stability (Δ_s), along the three paths shown in Fig. 1, by black dashed lines. We observe that these distances are linearly correlated [Figs. 4(a)–4(c)] for the molecular water models [green for ST2,[40] red for TIP4P/2005,[44,58] purple for TIP5P (supplementary material)], which means that for a system that exhibits a satisfactory level of collapse with the molecular water models, we can predict Δ_s given Δ_c (or vice versa). Thus, we attempt to locate the kinetic stability limit for real water using the linear correlation for molecular water models [Figs. 4(a)–4(c)] to predict the distance from the TMD line to the kinetic limit of liquid-vapor stability (Δ_s), given the distance from the LLCP to the TMD line (Δ_c) [blue triangles in Figs. 4(a)–4(c)], computed using the LLCP and thermodynamic property extrema given by the TSEOS fit.[59] The predicted kinetic liquid-vapor stability limit for real water is shown in Fig. 4(d) (blue triangles and the quadratic dotted-dashed fit) as well as the kinetic stability limits for molecular water models. We note that the location of the hypothesized LLCP in real water (shown in Fig. 2 at $T_c \approx 223$ K, $P_c \approx 42$ MPa) is highly uncertain [e.g., ($T_c \approx 232$ K, $P_c \approx 27$ MPa),[66] ($T_c \approx 223$ K, $P_c \approx 50$ MPa),[67] ($T_c \approx 227$ K, $P_c \approx 13$ MPa),[16] ($T_c \approx 168$ K, $P_c \approx 195$ MPa),[45]

($T_c \approx 210$ K, $P_c \approx 100$ MPa)[68], which strongly affects the prediction of the stability line (see Fig. S9 for how the prediction for the stability line shifts with the location of the LLCP).

The agreement between the experimental,[19] ST2[57], and TIP5P (supplementary material) kinetic stability limits shown in Fig. 4(d) is very satisfactory. At the same time, there is a clear disagreement between the experiments and both the kinetic stability limit the prediction for the TSEOS fit [based on the linear correlation shown in Figs. 4(a)–4(c)] and the TIP4P/2005,[44,58] calculations. Three implications follow from these facts. (1) The first, and the obvious, one is that the predictions are only as good as the models on which they are based. In particular, the TSEOS line [blue triangle locus in Fig. 4(d)] is the result of an extrapolation of the linear correlation [Figs. 4(a)–4(c)]. Furthermore, the kinetic stability limit predicted by the TSEOS model via the linear correlation is very sensitive to the location of the liquid-liquid critical point (Fig. S9). When the latter is obtained by parameter optimization, as in Fig. 2 (blue circle and associated loci), it is itself sensitive to the experimental data used in the optimization. (2) Second, the very concept of a kinetic spinodal is dependent on the time and length scales probed in experiments or simulations. Accordingly, the data shown in Fig. 4(d) represent an experimentally or computationally attained "limit" that reflects the technique used to probe the metastable liquid, rather than an immutable thermodynamic property. For example, the experimentally measured superheating limits of n-hexane show a clear dependence on the experimental technique (pulse heating, droplet superheating) used.[69,70] A further example is the difference between the cavitation of TIP4P/2005 as reported in Fig. 4(d)[44,58] (e.g., ca. −230 MPa, 300 K) and the estimate reported by Menzl *et al.* for the same system at a similar temperature, based on rate calculations[71] (ca. −126 MPa at 296.4 K). (3) Third, the correlation demonstrated in Figs. 4(a)–4(c) implies the existence of a relationship between vapor-liquid and liquid-liquid criticality in polyamorphic substances. This, we believe, is a significant observation, whose deeper implications deserve further study and exploration, independently of the correlation's model-dependent ability to predict kinetic stability "limits."

In light of the above considerations, the question naturally arises: can we use this finding of a correlation between liquid-liquid and vapor-liquid criticality to predict the thermodynamic vapor-liquid spinodal (an immutable property)? In what follows, we address this question for the van der Waals and lattice gas two-state theoretical models,[25] for which the thermodynamic vapor-liquid spinodal is known. As we show below (van der Waals) and in the supplementary material (lattice gas), the result is promising.

For the above-mentioned models, which are based on the underlying picture of interconversion between alternative molecular states, we kept the Widom line and the absolute liquid-vapor stability limit constant by fixing the liquid-vapor critical point and the energy, volume, and entropy parameters in Eq. (1) and constructed several scenarios by tuning the location of the LLCP along the Widom line by changing the nonideality in the Gibbs energy of mixing (see Anisimov *et al.*[25] for details). Upon applying the same rescaling procedure, we observed similar correlations between the distance from the LLCPs to the TMD line (Δ_c) and the distance from the TMD line to the liquid-vapor spinodal (Δ_s) along several paths, as shown in Fig. 5(a) for the van der Waals model. Particularly, for the simple fluid models, we define the three paths along L1, L3, and the Widom line (Fig. 1). The liquid vapor spinodal for these fluid models is constructed accurately from the observed correlations, as shown in Fig. 5(b). Similar results are given for the lattice-gas model in Fig. S10 in the supplementary material.

We note that the correlation between the distance to the LLCP and the liquid-vapor stability limit, and, more broadly, the interdependence of liquid-vapor and liquid-liquid transitions can be explained by considering the two-state formulation of polyamorphic fluids where the fluid is defined by the existence of two interconvertible states, A and B.[22,25] In particular, in the thermodynamics of two competing structures,[22,25] the shape of the liquid-liquid transition line, the slope of the Widom line, and the location of LLCP are defined by the difference in the Gibbs energies between states B and A, while the shape of TMD is also affected by state A. Specifically, since the vapor-liquid spinodal is a part of state A,[22] the anomalous behavior of the state A's density near the liquid-vapor spinodal modifies the shape of TMD significantly.

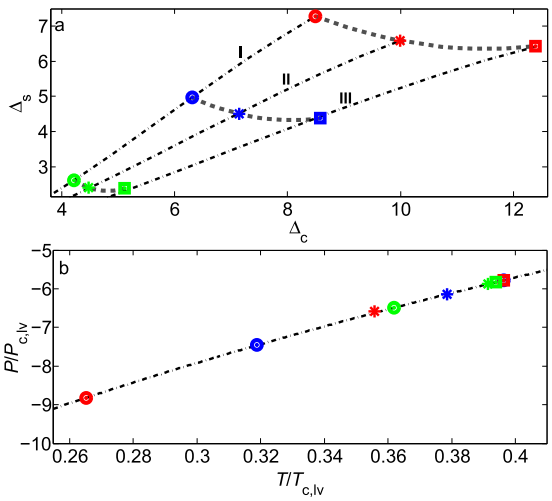

FIG. 5. The correlation between the location of the liquid-liquid critical point, the locus of density extrema, and the liquid-vapor spinodal (LVS) upon tuning the location of the liquid-liquid critical point for the two-state van der Waals model. (a) Δ_c is the distance between LLCP and the points at which the density extrema intersect the locus of κ_T extrema (I); the Widom line (II), and the locus of C_P extrema (III). Δ_s is the distance between the liquid stability lines and points on density extrema loci along the same paths. (b) The reconstruction of the LVS from the correlations between Δ_c and Δ_s (green, blue, and red symbols correspond to three different values of the LLCP). $T_{c,lv}$ and $P_{c,lv}$ are the pressure and temperature of the LVCP. The dotted-dashed line is the liquid-vapor spinodal for the two-state van der Waals model.

A correlation between the location of the LLCP, the shape of the TMD line, and the liquid-vapor kinetic spinodal is a generic feature of polyamorphic fluids. The quantitative correlation along three selected paths, suggested and verified in this work, is very simple (linear or very close to linear). It works well for three molecular water models. However, our procedure, in the specific form in which it has been formulated, cannot be generally applicable to polymorphic fluids with very different LLPT topologies. For example, when the slope of line L1 is less negative than that of the line joining the liquid-liquid and liquid-vapor critical points, L1 will not cross the liquid-vapor kinetic spinodal, and thus, this particular path cannot be used in the prediction of LVS. Furthermore, the procedure fails in two special cases: the "bird's beak" in the LL coexistence[25] and a vertical LLPT. In both cases, the TMD line collapses or disappears. Extension of our method so as to encompass these cases may necessitate modifications in the form of the correlation and/or the scaling procedure and would require additional studies.

IV. CONCLUSION

We present a rescaling of the thermodynamic property extrema of previously published and new simulation results for three commonly used molecular models of water (ST2,[38,57,60] TIP4P/2005,[44,58] and TIP5P). The rescaling procedure results in a satisfactory near-collapse of the property extrema loci for these three models. The rescaled coordinates bring forth an intriguing correlation between the location of the liquid-liquid critical point, the line of density extrema, and the *kinetic* stability limit of the liquid state with respect to the vapor (cavitation line). This underlines the interdependence of liquid-liquid and liquid-vapor transitions in polyamorphic fluids. Our results are supported by similar correlations between the location of the liquid-liquid critical point, the line of density extrema, and the *thermodynamic* stability limit of the liquid state with respect to the vapor for two generic models that also exhibit a second critical point, namely, the van der Waals and lattice-gas "two-state" models. We utilize this general trend to predict the *kinetic* stability limit of the liquid state in simultaneously supercooled and stretched water, for which experimental data are currently unavailable. We note that the general trend identified in this work could also be potentially utilized for the prediction of the thermodynamic stability limit for real water by constructing the liquid-vapor spinodals for the water models and establishing similar correlations between them. The thermodynamic stability limit is not directly attainable, but there are theoretical studies that investigate the relationship between the kinetic and thermodynamic stability limits of water,[9,22,71] and future work could utilize these studies to investigate the liquid-vapor spinodal for real water. It will be also interesting to explore the extent to which the present scaling procedure can be successfully applied to other tetrahedral systems exhibiting water-like behavior, such as tetrahedral patchy colloids,[72] silicon,[29–31] and silica.[32] We plan to pursue such studies in the future.

SUPPLEMENTARY MATERIAL

See supplementary material for simulation details, the phase diagram for TIP5P, and the thermodynamic property extrema profiles for TIP4P/2005, ST2, and TIP5P water models.

ACKNOWLEDGMENTS

We acknowledge John Biddle, Michal Duška, Frédéric Caupin, Giancarlo Franzese, and Valeria Molinero for helpful discussions. We thank Peter Poole and Rakesh Singh for providing us simulation data on ST2 and TIP4P/2005, respectively. This work used the Extreme Science and Engineering Discovery Environment (XSEDE), which is supported by the National Science Foundation Grant No. ACI-1548562. M.A.A. acknowledges the financial support of the American Chemical Society Petroleum Research Fund (Grant No. 59434-ND6). Simulations of TIP5P were performed at the Terascale Infrastructure for Groundbreaking Research in Science and Engineering (TIGRESS) high performance computer center at Princeton University.

REFERENCES

[1] R. J. Speedy and C. A. Angell, J. Chem. Phys. **65**, 851 (1976).
[2] C. A. Angell, W. J. Sichina, and M. Oguni, J. Phys. Chem. **86**, 998 (1982).
[3] D. E. Hare and C. M. Sorensen, J. Chem. Phys. **84**, 5085 (1986).
[4] P. H. Poole, F. Sciortino, U. Essmann, and H. E. Stanley, Nature **360**, 324 (1992).
[5] P. H. Poole, F. Sciortino, T. Grande, H. E. Stanley, and C. A. Angell, Phys. Rev. Lett. **73**, 1632 (1994).
[6] O. Mishima and H. E. Stanley, Nature **392**, 164 (1998).
[7] A. K. Soper and M. A. Ricci, Phys. Rev. Lett. **84**, 2881 (2000).
[8] H. Tanaka, Phys. Rev. B **66**, 064202 (2002).
[9] F. Caupin, Phys. Rev. E **71**, 051605 (2005).
[10] F. Caupin and E. Herbert, C. R. Phys. **7**, 1000 (2006).
[11] K. Winkel, M. S. Elsaesser, E. Mayer, and T. Loerting, J. Chem. Phys. **128**, 044510 (2008).
[12] K. Stokely, M. G. Mazza, H. E. Stanley, and G. Franzese, Proc. Natl. Acad. Sci. U. S. A. **107**, 1301 (2010).
[13] G. Franzese and H. Stanley, *Water and Life* (CRC Press, 2010), pp. 101–117.
[14] G. N. I. Clark, G. L. Hura, J. Teixeira, A. K. Soper, and T. Head-Gordon, Proc. Natl. Acad. Sci. U. S. A. **107**, 14003 (2010).
[15] E. B. Moore and V. Molinero, Nature **479**, 506 (2011).
[16] V. Holten and M. A. Anisimov, Sci. Rep. **2**, 713 (2012).
[17] C. A. Angell, Nat. Mater. **13**, 673 (2014).
[18] P. Gallo, K. Amann-Winkel, C. A. Angell, M. A. Anisimov, F. Caupin, C. Chakravarty, E. Lascaris, T. Loerting, A. Z. Panagiotopoulos, J. Russo, J. A. Sellberg, H. E. Stanley, H. Tanaka, C. Vega, L. Xu, and L. G. M. Pettersson, Chem. Rev. **116**, 7463 (2016).
[19] C. Qiu, Y. Krüger, M. Wilke, D. Marti, J. Rička, and M. Frenz, Phys. Chem. Chem. Phys. **18**, 28227 (2016).
[20] Q. Zheng, D. J. Durben, G. H. Azouzi, and C. A. Angell, Science **254**, 829 (1991).
[21] M. E. M. Azouzi, C. Ramboz, J.-F. Lenain, and F. Caupin, Nat. Phys. **9**, 38 (2012).
[22] J. W. Biddle, R. S. Singh, E. M. Sparano, F. Ricci, M. A. González, C. Valeriani, J. L. F. Abascal, P. G. Debenedetti, M. A. Anisimov, and F. Caupin, J. Chem. Phys. **146**, 034502 (2017).

[23]V. Holten, C. Qiu, E. Guillerm, M. Wilke, J. Rička, M. Frenz, and F. Caupin, J. Phys. Chem. Lett. **8**, 5519 (2017).
[24]Y. E. Altabet, R. S. Singh, F. H. Stillinger, and P. G. Debenedetti, Langmuir **33**, 11771 (2017).
[25]M. A. Anisimov, M. Duška, F. Caupin, L. E. Amrhein, A. Rosenbaum, and R. J. Sadus, Phys. Rev. X **8**, 011004 (2018).
[26]M. A. Morales, C. Pierleoni, E. Schwegler, and D. M. Ceperley, Proc. Natl. Acad. Sci. U. S. A. **107**, 12799 (2010).
[27]M. Zaghoo, A. Salamat, and I. F. Silvera, Phys. Rev. B **93**, 155128 (2016).
[28]P. Dalladay-Simpson, R. T. Howie, and E. Gregoryanz, Nature **529**, 63 (2016).
[29]V. V. Vasisht and S. Sastry, in *Liquid Polymorphism* (John Wiley & Sons, Inc., 2013), pp. 463–517.
[30]S. Sastry and C. A. Angell, Nat. Mater. **2**, 739 (2003).
[31]G. Zhao, J. L. Yan, Y. J. Yu, M. C. Ding, X. G. Zhao, and H. Y. Wang, Sci. Rep. **7**, 39952 (2017).
[32]R. Chen, E. Lascaris, and J. C. Palmer, J. Chem. Phys. **146**, 234503 (2017).
[33]I. Saika-Voivod, F. Sciortino, T. Grande, and P. H. Poole, Phys. Rev. E **70**, 061507 (2004).
[34]J. N. Glosli and F. H. Ree, Phys. Rev. Lett. **82**, 4659 (1999).
[35]A. Cadien, Q. Y. Hu, Y. Meng, Y. Q. Cheng, M. W. Chen, J. F. Shu, H. K. Mao, and H. W. Sheng, Phys. Rev. Lett. **110**, 125503 (2013).
[36]Y. Katayama, T. Mizutani, W. Utsumi, O. Shimomura, M. Yamakata, and K. ichi Funakoshi, Nature **403**, 170 (2000).
[37]K. Amann-Winkel, C. Gainaru, P. H. Handle, M. Seidl, H. Nelson, R. Bohmer, and T. Loerting, Proc. Natl. Acad. Sci. U. S. A. **110**, 17720 (2013).
[38]F. Smallenburg, P. H. Poole, and F. Sciortino, Mol. Phys. **113**, 2791 (2015).
[39]J. C. Palmer, F. Martelli, Y. Liu, R. Car, A. Z. Panagiotopoulos, and P. G. Debenedetti, Nature **510**, 385 (2014).
[40]P. H. Poole, R. K. Bowles, I. Saika-Voivod, and F. Sciortino, J. Chem. Phys. **138**, 034505 (2013).
[41]Y. Liu, J. C. Palmer, A. Z. Panagiotopoulos, and P. G. Debenedetti, J. Chem. Phys. **137**, 214505 (2012).
[42]J. C. Palmer, R. Car, and P. G. Debenedetti, Faraday Discuss. **167**, 77 (2013).
[43]Y. Li, J. Li, and F. Wang, Proc. Natl. Acad. Sci. U. S. A. **110**, 12209 (2013).
[44]R. S. Singh, J. W. Biddle, P. G. Debenedetti, and M. A. Anisimov, J. Chem. Phys. **144**, 144504 (2016).
[45]Y. Ni and J. L. Skinner, J. Chem. Phys. **144**, 214501 (2016).
[46]H. Pathak, J. C. Palmer, D. Schlesinger, K. T. Wikfeldt, J. A. Sellberg, L. G. M. Pettersson, and A. Nilsson, J. Chem. Phys. **145**, 134507 (2016).
[47]L. Xu, P. Kumar, S. V. Buldyrev, S.-H. Chen, P. H. Poole, F. Sciortino, and H. E. Stanley, Proc. Natl. Acad. Sci. U. S. A. **102**, 16558 (2005).
[48]J. C. Palmer, P. H. Poole, F. Sciortino, and P. G. Debenedetti, Chem. Rev. **118**, 9129 (2018).
[49]V. Molinero and E. B. Moore, J. Phys. Chem. B **113**, 4008 (2009).
[50]J. Lu, C. Chakravarty, and V. Molinero, J. Chem. Phys. **144**, 234507 (2016).
[51]D. Dhabal, C. Chakravarty, V. Molinero, and H. K. Kashyap, J. Chem. Phys. **145**, 214502 (2016).
[52]F. H. Stillinger and A. Rahman, J. Chem. Phys. **60**, 1545 (1974).
[53]J. L. F. Abascal and C. Vega, J. Chem. Phys. **123**, 234505 (2005).
[54]M. Lísal, I. Nezbeda, and W. R. Smith, J. Phys. Chem. B **108**, 7412 (2004).
[55]V. V. Vasisht and S. Sastry, "Liquid-liquid phase transition in supercooled silicon," in *Liquid Polymorphism*, edited by S. A. Rice, A. R. Dinner, and H. E. Stanley (2013), pp. 463–517.
[56]M. H. Bhat, V. Molinero, E. Soignard, V. C. Solomon, S. Sastry, J. L. Yarger, and C. A. Angell, Nature **448**, 787 (2007).
[57]P. H. Poole, I. Saika-Voivod, and F. Sciortino, J. Phys.: Condens. Matter **17**, L431 (2005).
[58]M. A. González, C. Valeriani, F. Caupin, and J. L. F. Abascal, J. Chem. Phys. **145**, 054505 (2016).
[59]M. Duška, J. Hrubý, F. Caupin, and M. A. Anisimov, e-print arXiv:1708.04054 [physics.chem-ph] (2017).
[60]F. Sciortino, I. Saika-Voivod, and P. H. Poole, Phys. Chem. Chem. Phys. **13**, 19759 (2011).
[61]P. G. Debenedetti, *Metastable Liquids. Concepts and Principles* (Princeton University Press, 1996).
[62]S. Sastry, P. G. Debenedetti, F. Sciortino, and H. E. Stanley, Phys. Rev. E **53**, 6144 (1996).
[63]E. A. Guggenheim, J. Chem. Phys. **13**, 253 (1945).
[64]T. W. Leland and P. S. Chappelear, Ind. Eng. Chem. **60**, 15 (1968).
[65]J. Biddle, "Two-state thermodynamics of supercooled water," Ph.D. dissertation (University of Maryland, College Park, 2016), pp. 233–235.
[66]D. A. Fuentevilla and M. A. Anisimov, Phys. Rev. Lett. **97**, 195702 (2006).
[67]O. Mishima, J. Chem. Phys. **133**, 144503 (2010).
[68]N. J. Hestand and J. L. Skinner, J. Chem. Phys. **149**, 140901 (2018).
[69]V. Skripov and G. Ermakov, Russ. J. Phys. Chem. **38**, 208 (1964).
[70]V. Skripov and G. Ermakov, High Temp. **8**, 540 (1970), available at http://mi.mathnet.ru/eng/tvt7669.
[71]G. Menzl, M. A. Gonzalez, P. Geiger, F. Caupin, J. L. F. Abascal, C. Valeriani, and C. Dellago, Proc. Natl. Acad. Sci. U. S. A. **113**, 13582 (2016).
[72]F. Smallenburg, L. Filion, and F. Sciortino, Nat. Phys. **10**, 653 (2014).